Finite range calculations of light-ion two-neutron transfer reactions*

L. A. Charlton
Department of Physics, The Florida State University, Tallahassee, Florida 32306
(Received 18 February 1975)

A full finite-range distorted-wave Born-approximation formalism is used to calculate the two-neutron transfer reactions $^{18}O(p,t)^{16}O$(g.s.), $^{40}Ca(t,p)^{42}Ca$(g.s.), and $^{208}Pb(p,t)^{206}Pb$(g.s.). It is found that the shape of the differential cross section is well predicted in the forward direction for all nuclei studied, but the normalization is given correctly only for ^{18}O.

[NUCLEAR REACTIONS $^{18}O(p,t)$, $E=20$ MeV; $^{40}Ca(t,p)$, $E=10.1$ MeV; $^{208}Pb(p,t)$, $E=35$ MeV; ground state transitions. Calculated $\sigma(\theta)$. Finite-range DWBA.]

I. INTRODUCTION

Light-ion-induced two-nucleon transfer reaction data are almost always analyzed with the use of distorted-wave Born approximation (DWBA) and the zero-range approximation. Theoretical work which tests the validity of the zero-range approximation includes the work of Bayman,[1] Bayman and Feng,[2] and Takemasa.[3] In the first two references exact finite-range calculations are performed only for a pure configuration transfer. The methodology of Ref. 3 also involves a full finite-range calculation but uses a somewhat unphysical Gaussian form for the triton wave function. The purpose of this paper is to report a study of two-neutron transfer reactions. A full finite-range DWBA formalism is used which allows a coherent sum of all components of the two-neutron wave function and also uses a realistic description of the triton.

Only ground state transitions in which the target or residual nucleus is a doubly closed shell nucleus are considered. The configuration space allowed includes all relevant components from the major shell above (or below) the closed shell nuclei involved.

II. FORMALISM

The calculational methods used here are similar to those of Ref. 4. The distorted waves are expanded in plane waves[9-11] and the single-nucleon orbitals are expanded in harmonic oscillator functions.[5] The use of a Moshinsky transformation[6] then allows the DWBA triple vector integral to be written as a sum over single integrals.

A two-neutron transfer reaction can be written as

$$p+T\rightarrow t+R\ ,$$

$$T=R+H\ ,$$

$$t=p+H\ ,$$

and

$$H=n_1+n_2\ .$$

For such a process the differential cross section using DWBA, is

$$\frac{d\sigma_{pt}}{d\Omega}=\frac{m_{pT}m_{tR}}{(2\pi\hbar^2)^2}\frac{k_t}{k_p}\hat{j}_t^{-2}\hat{J}_T^{-2}\sum_{M_R\mu_t}\sum_{M_T\mu_p}|T_{M_R\mu_t M_T\mu_p}|^2 \tag{2.1}$$

with

$$T_{M_R\mu_t M_T\mu_p}=C(T_R1T_T;N_R1N_T)\times\sum_{J_{HR}}\int d\vec{r}_{pH}d\vec{r}_{HR}d\vec{r}_{n_1n_2}d\xi_R\chi_t^{(-)\dagger}(k_t,\vec{r}_{tR})\chi^{J_R^\dagger}_{M_R}(\xi_R)\chi^{j_t^\dagger}_{\mu_t}V_{pH}[\Psi^{J_{HR}}\chi^{J_R}(\xi_R)]^{J_T}_{M_T}\eta^{1/2}_{\mu_p}(\sigma_p)\chi_p^{(+)}(\vec{k}_p,\vec{r}_{pT})\ . \tag{2.2}$$

In the above,

$$\chi^{j_t}_{\mu_t}=\theta(\vec{r}_{n_1n_2},\vec{r}_{pH})[\eta^{1/2}(\sigma_1)\eta^{1/2}(\sigma_2)]^0_0\eta_{\mu_t}{}^{1/2}(\sigma_p)\ , \tag{2.3}$$

χ_p and χ_t are distorted waves, the T's are isospin quantum numbers with projections N,

$$V_{pH}=V_{n_1}(|\vec{r}_{n_1p}|)+V_{n_2}(\vec{r}_{n_2p}|)\ , \tag{2.4}$$

and

$$\Psi^{J_{HR}} = \sum_{n_1 l_1 j_1} \sum_{n_2 l_2 j_2} A^{j_1 j_2 J_{HR}}_{n_1 n_2 l_1 l_2} \frac{[\Phi^{n_1 l_1 j_1}(\vec{r}_{n_1 R}, \sigma_1)\Phi^{n_2 l_2 j_2}(\vec{r}_{n_2 R}, \sigma_2)]^{J_{HR}}_{J_{HR}} - [\Phi^{n_1 l_1 j_1}(\vec{r}_{n_2 R}, \sigma_2)\Phi^{n_2 l_2 j_2}(\vec{r}_{n_1 R}, \sigma_1)]^{J_{HR}}_{M_{HR}}}{[2(1+\delta_{n_1 n_2}\delta_{l_1 l_2}\delta_{j_1 j_2})]^{1/2}} . \quad (2.5)$$

The specific form for the transfer potential used in the calculations presented later was[7]

$$V_{n_i}(r) = \infty \quad (r < r_c)$$
$$= V_0 e^{-2.5(r-r_c)} \quad (r > r_c)$$

with $V_0 = -481.21$ MeV and $r_c = 0.45$ fm. Since the above form is spin independent, only the dineutron singlet spin state is included. The triplet contribution would be expected to be small.[1,3]

In Eq. (2.5), the single-particle orbitals are

$$\Phi^{nlj}_m(\vec{r}, \sigma) = [\phi^{nl}(\vec{r})\eta^{1/2}(\sigma)]^j_m \quad (2.6)$$

with

$$\phi^{nl}_m(\vec{r}) = (i)^l u_{nl}(r) Y^l_m(\hat{\vec{r}}) \quad (2.7)$$

and the A is a spectroscopic amplitude. The coordinates are related by

$$\vec{r}_{pT} = \vec{r}_{pH} + m_R m_T^{-1}\vec{r}_{HR} ,$$
$$\vec{r}_{tR} = \vec{r}_{HR} + m_p m_t^{-1}\vec{r}_{pH} ,$$
$$\vec{r}_{pH} = -\tfrac{1}{2}(\vec{r}_{pn_1} + \vec{r}_{pn_2}) , \quad (2.8)$$
$$\vec{r}_{HR} = \tfrac{1}{2}(\vec{r}_{n_1 R} + \vec{r}_{n_2 R}) ,$$

and

$$\vec{r}_{n_1 n_2} = \vec{r}_{pn_1} - \vec{r}_{pn_2} = \vec{r}_{n_1 R} - \vec{r}_{n_2 R} .$$

It is now desired to transform all coordinates into those to be averaged in Eq. (2.2). The spatial part of the single-particle wave function pairs of Eq. (2.5) are expanded in oscillator functions.[5] This gives

$$[\Phi^{n_1 l_1 j_1}(\vec{r}_{n_i R}, \sigma_i)\Phi^{n_2 l_2 j_2}(\vec{r}_{n_j R}, \sigma_j)]^{J_{HR}}_{M_{HR}} = \sum_{\tilde{n}_1 \tilde{n}_2} a_{\tilde{n}_1} a_{\tilde{n}_2} [\tilde{\Phi}^{\tilde{n}_1 l_1 j_1}(\vec{r}_{n_i R}, \sigma_i) \times \tilde{\Phi}^{\tilde{n}_2 l_2 j_2}(\vec{r}_{n_j R}, \sigma_j)]^{J_{HR}}_{M_{HR}} , \quad (2.9)$$

where i and j are 1 or 2, $\tilde{\Phi}$ contains a harmonic oscillator radial wave function (but is otherwise identical to Φ), and the a's are overlaps of Φ and $\tilde{\Phi}$. Transforming from j-j to L-S coupling and performing a Moshinsky transformation[6] allows Eq. (2.9) to be written as

$$[\Phi^{n_1 l_1 j_1}(\vec{r}_{n_i R}, \sigma_i)\Phi^{n_2 l_2 j_2}(\vec{r}_{n_j R}, \sigma_j)]^{J_{HR}}_{M_{HR}} = \sum_{LS} \sum_{\tilde{n}_1 \tilde{n}_2} \sum_{\tilde{n}\tilde{l}\,\tilde{N}\tilde{\mathfrak{L}}} \hat{j}_1 \hat{j}_2 \hat{L} \hat{S} a_{\tilde{n}_1} a_{\tilde{n}_2} \times \begin{Bmatrix} l_1 & \frac{1}{2} & j_1 \\ l_2 & \frac{1}{2} & j_2 \\ L & S & J_{HR} \end{Bmatrix} \langle \tilde{n}\tilde{l}, \tilde{N}\tilde{\mathfrak{L}}, L \,|\, \tilde{n}_1 l_1, \tilde{n}_2 l_2 L \rangle \times \{[\tilde{\phi}^{\tilde{n}\tilde{l}}(\vec{r}_{n_1 n_2})\tilde{\phi}^{\tilde{N}\tilde{\mathfrak{L}}}(\vec{r}_{HR})]^L [\eta^{1/2}(\sigma_1)\eta^{1/2}(\sigma_2)]^S\}^{J_{HR}}_{M_{HR}} . \quad (2.10)$$

The triton spatial wave function of Eq. (2.3) is assumed to be symmetric, have orbital angular momentum zero, and have the form

$$\theta(\vec{r}_{n_1 n_2}, \vec{r}_{pH}) = N\rho(|\vec{r}_{n_1 n_2}|)\rho(|\vec{r}_{n_1 p}|)\rho(|\vec{r}_{n_2 p}|) . \quad (2.11)$$

The ρ's were taken to have the form

$$\rho(r) = g(r)f(r) ,$$

where

$$g(r) = (e^{-ar} - e^{-br})/r^{1/2} ,$$
$$f(r) = 1 - \exp\{-c[(r/r_a)^2 - 1]\} ,$$
$$a = 0.275 \text{ fm}^{-1} ,$$
$$b = 1.525 \text{ fm}^{-1} ,$$
$$r_c = 0.45 \text{ fm} ,$$

and

$$c = 0.376 .$$

The g function was found in Ref. 8 to have a correct asymptotic form and f takes the wave function smoothly to zero at a "hard core" radius of 0.45 fm.[26]

In order to achieve the stated objective of transforming to the coordinates to be averaged in the DWBA integral, both the triton wave function [Eq. (2.11)] and the product of the triton wave function and the transfer potential [Eq. (2.4)] must be expanded in oscillator functions. This gives

$$[V_{n_1}(r_{n_1p})+V_{n_2}(r_{n_2p})]\rho(r_{n_1n_2})\rho(r_{n_1p})\rho(r_{n_2p})=\rho(r_{n_1n_2})\sum_{\tilde{n}_1^t\tilde{n}_2^t}[a_{\tilde{n}_1^t}a'_{\tilde{n}_2^t}+a'_{\tilde{n}_1^t}a_{\tilde{n}_2^t}][\tilde{\phi}^{\tilde{n}_1^t0}(\vec{r}_{n_1p})\tilde{\phi}^{\tilde{n}_2^t0}(\vec{r}_{n_2p})]_0^0\,, \tag{2.12}$$

where the a's are overlaps between ρ and $\tilde{\phi}$ and the a''s are overlaps between $V\rho$ and $\tilde{\phi}$. A Moshinsky transformation now yields, for Eq. (2.12),

$$\rho(r_{n_1n_2})\sum_{\tilde{n}_1^t\tilde{n}_2^t}[a_{\tilde{n}_1^t}a'_{\tilde{n}_2^t}+a'_{\tilde{n}_1^t}a_{\tilde{n}_2^t}]\langle\tilde{n}^t\tilde{l}^t,\tilde{N}^t\tilde{l}^t,0|\tilde{n}_1^t0,\tilde{n}_2^t0,0\rangle[\tilde{\phi}^{\tilde{n}^t\tilde{l}^t}(\vec{r}_{n_1n_2})\tilde{\phi}^{\tilde{N}^t\tilde{l}^t}(\vec{r}_{pH})]_0^0\,. \tag{2.13}$$

Thus, all bound states quantities now contain only the desired coordinates. The distorted waves may be transformed into a form in which they contain only $\vec{r}_{pH}$ and $\vec{r}_{HR}$ by means of the plane wave expansions of Refs. 9 and 10. Further, all calculational techniques of Ref. 10 may now be used and yield the final form for the cross section given in the Appendix. The computer program MERCURY[10,11] was modified to perform the numerical calculations. The modification essentially consisted of replacing the form factors of single-particle transfer with the series of form factors given by Eqs. (A9) and (A10).

It should be noted that the amount of computing required is somewhat independent of the number of configurations used since the sum over the quantum numbers defining each configuration is done in Eq. (A10). As noted in Ref. 4 only a few values of $\tilde{l}$ in Eq. (A2) need to be included. In the results presented later only $\tilde{l}=0,2$ were used ($\tilde{l}=1$ is excluded). The larger value of $\tilde{l}$ made only a small contribution to the calculated cross section. Small values of $\tilde{l}$ imply small values for $\tilde{\mathcal{L}}$ also through the selection rules on the Moshinsky bracket in Eq. (A10). It was also reported in Ref. 4 that only a limited range of $\tilde{n}$ and $\tilde{n}^t$ are required. Only $\tilde{n}$ (or $\tilde{n}^t$) = 0, 1 were used here. Again the larger values contributed little to the cross section.

III. RESULTS

Numerical calculations were performed for (p,t) reactions on ^{18}O and ^{208}Pb and also for (t,p) on ^{40}Ca. These three nuclei were chosen because of the availability of structure information and because they might be expected to have fairly simple shell model wave functions since the two neutrons are added to (or taken from) doubly closed shell nuclei. In the case of ^{40}Ca, full finite-range calculations have already been done by Bayman[1] and by Bayman and Feng[2] for a single configuration only. This allowed a check on the numerics. Ground state transitions only are presented in this paper.

The optical potentials used for the distorted waves had the form

$$V(r)=V_C(r)-Vf_v(r)-iWf_w(r)+4ia_wW_Df'_D(r)\,, \tag{3.1}$$

where

$$f_x=\{1+\exp[(r-r_xA^{1/3})/a_x]\}^{-1} \tag{3.2}$$

and V_C is a Coulomb potential due to a uniformly charged sphere of radius $r_cA^{1/3}$. The optical parameters used for the protons are shown in Table I and those for the tritons in Table II. Bound neutron orbitals were generated from a potential of the form

$$V(r)=V_Bf_v(r)+V_B\frac{\lambda}{45.2}\frac{1}{r}\frac{d}{dr}f_v(r)\vec{L}\cdot\vec{S} \tag{3.3}$$

with f_v given by Eq. (3.2), $r_v=1.25$, $a_v=0.65$, $\lambda=25$, and V_B varied to give the correct asymptotic form. The spectroscopic amplitudes used [the A's in Eq. (2.5)] are given in Table III.

In Fig. 1 the differential cross section for ^{18}O-$(p,t)^{16}$O(g.s.) is shown. Optical parameter sets

TABLE I. Proton optical parameters.

Nucleus and set	V	W	W_D	r_c	r_v	a_v	r_w	a_w	Ref.
^{18}O-P1	53.6	1.5	6.0	1.25	1.07	0.74	1.34	0.64	12
^{18}O-P2	56.0	1.7	0	1.25	1.17	0.75	1.32	0.588	12
^{42}Ca	53.0	0	15.5	1.25	1.25	0.65	1.25	0.47	13
^{208}Pb	53.4	5.0	5.6	1.17	1.17	0.75	1.32	0.66	19

TABLE II. Triton optical parameters.

Nucleus and set	V	W	W_D	r_c	r_v	a_v	r_w	a_w	Ref.
^{16}O-T1	170.58	9.75	0	1.16	1.16	0.66	1.90	0.8	12
^{16}O-T2	146.8	14.7	0	1.4	1.4	0.44	1.4	0.551	12
^{40}Ca	144.0	30.0	0	1.24	1.24	0.678	1.45	0.841	13
^{206}Pb	167.0	10	0	1.16	1.16	0.75	1.50	0.820	20

P1 and T1 were used. These sets were found in the reference cited to match elastic scattering. It is seen that the DWBA calculations match both the shape and the normalization of the data in the forward direction when either a $(2s_{1/2})^2$-$(1d_{5/2})^2$ configuration space is used or full s-d shell description is included. The use of a pure $(1d_{5/2})^2$ configuration gives the same shape but underpredicts the cross section at the forward angles by about a factor of 3. The second maxima in the calculations is too small. However, a $(2s_{1/2})^2$-$(1d_{5/2})^2$ configuration space differs from one set of data by about the same amount as the two sets of data differ from each other. Backward of ~60° the calculations give a poor description of the data in both shape and normalization. Over all, the two or the three component wave functions give excellent results in the extreme forward direction but fall off too rapidly.

In Fig. 2 a calculation for the same process is shown, but optical parameter sets P2 and T2 were used. These two sets were found in Ref. 12 to give the best fit to the transfer data in a zero-range calculation. The normalization of the full finite-range calculation of Fig. 2 is as shown. The optical parameters used, however, do not match elastic scattering. Also, the calculated cross section is much too large in the extreme forward direction (compare with Fig. 1). Thus, the results of Fig. 2 are regarded as no more than a parametrization of the data and are shown to illustrate this point.

In Fig. 3, the differential cross section for ^{40}Ca-$(t,p)^{42}$Ca(g.s.) is shown. The pure configuration transfer calculation is a repeat of a result in Ref. 1. The use of a single component wave function gives a cross section strength that is ~40% too

TABLE III. Spectroscopic amplitudes.

		^{18}O		
$(1d_{5/2})^2$	$(2s_{1/2})^2$		$(1d_{3/2})^2$	Ref.
0.952	0.270		0.146	21
0.893	0.450		···	22
1.0	···		···	
		^{42}Ca		
$(2p_{3/2})^2$	$(1f_{7/2})^2$	$(1f_{5/2})^2$	$(2p_{1/2})^2$	Ref.
0.22	0.97	0.14	0.11	13
1.0	···	···	···	···
		^{208}Pb		
$(3p_{1/2})^{-2}$	$(2f_{5/2})^{-2}$		$(3p_{3/2})^{-2}$	Ref.
0.832	0.416		0.379	23
1.0	···		···	···

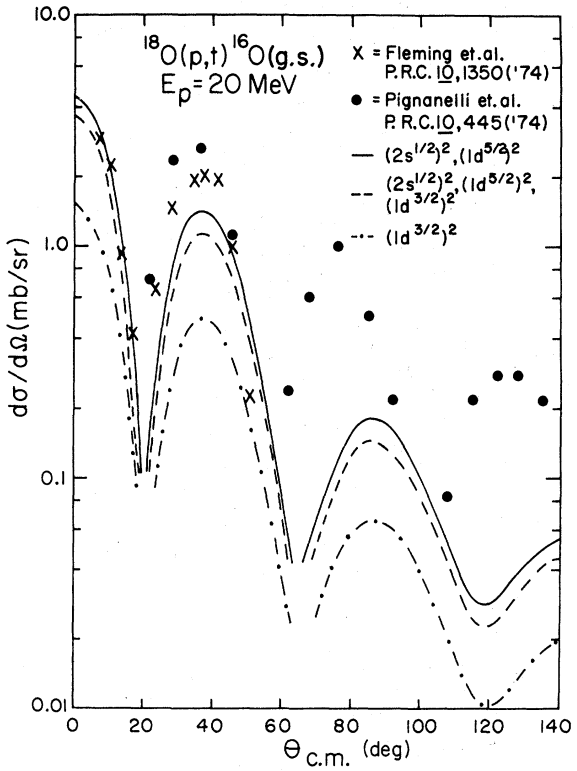

FIG. 1. Differential cross section for $^{18}O(p,t)^{16}O$(g.s.). The effect produced by using a one-, two-, or three-component wave function for ^{18}O is illustrated. The normalization of the calculated cross sections is as shown. Optical parameter sets P1 and T1 were used. Symbols are as follows: ×, D. Fleming *et al.*, Phys. Rev. C 10, 1350, (1974); ●, M. Pignanelli *et al.*, Phys. Rev. C 10, 445 (1974); —, $(2s_{1/2})^2$, $(1d_{5/2})^2$; ---, $(2s_{1/2})^2$, $(1d_{5/2})^2$, $(1d_{3/2})^2$; -·-, $(1d_{3/2})^2$.

small. Including a full f-p shell configuration space makes the normalization worse by more than a factor of 2. This is due to the large $(2p_{3/2})^2$ DWBA matrix element relative to the $(1f_{7/2})^2$. Including the entire f-p shell takes the transfer from pure $(2p_{3/2})^2$ to almost pure $(1f_{7/2})^2$ (see Table III). This loss of strength is consistent with the estimates of Ref. 1. It would probably be possible to arbitrarily assign weights to the various f-p components and get the experimental strength. Without structure justification, this again would be a parametrization of the data. The point is, however, that if some mechanism, not included in Ref. 13, were available that would greatly enhance the $(2p)^2$ spectroscopic amplitudes relative to the $(1f)^2$, the normalization problem would be less or nonexistent.

The shape of the calculated cross section in Fig. 3 has the same characteristics as that of Fig. 1 for $^{18}O(p,t)^{16}O$. That is, it fits very well in the extreme forward direction but falls off too rapidly.

In Fig. 4 the differential cross section is shown for $^{208}Pb(p,t)^{206}Pb$. The single configuration transfer underpredicts the cross section by a factor of 5.2. A three component wave function gives a strength about 3 times higher. The shape is in good agreement with the data. However, only forward angle data are available. The calculated strength of the transition is too low by about 40%.

For the three nuclei studied here, full finite-range DWBA gives an excellent description of the shape of the forward angle cross section. However, for the two nuclei where backward angle data were available, the calculated cross section falls off too rapidly. The normalization is in excellent agreement for ^{18}O and reasonable agreement for ^{208}Pb. For ^{42}Ca, however, the calculated strength is too low.

IV. DISCUSSION

The two most obvious omissions in the study of this paper are (1) only a direct one step process has been allowed, and (2) only a limited configuration space was used. Some work has been done by other authors which allows multistep pro-

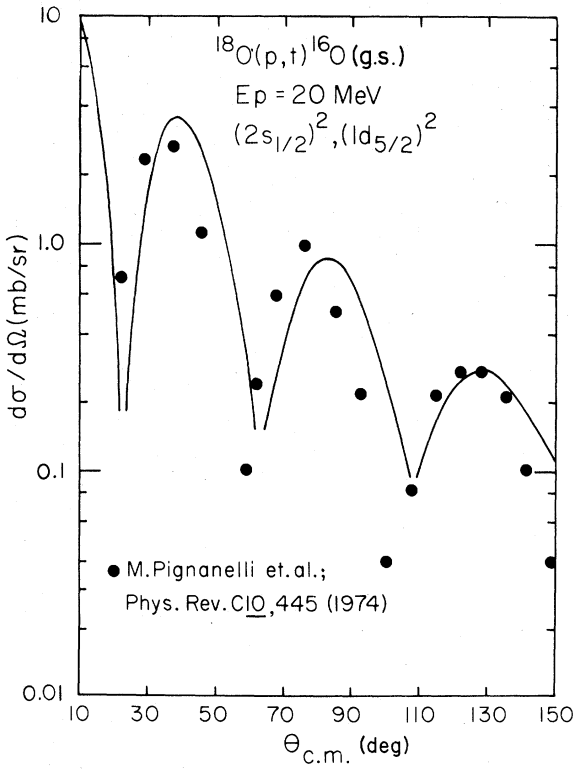

FIG. 2. Differential cross section for $^{18}O(p,t)^{16}O$(g.s.). Optical parameter sets P2 and T2 were used which were found in Ref. 12 to give the best fit for the transfer data. The normalization of the calculated cross section is as shown.

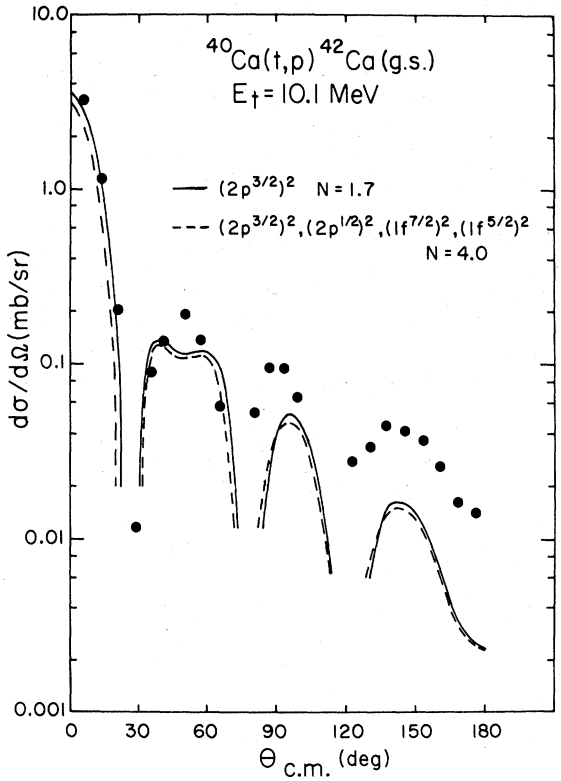

FIG. 3. Differential cross section for $^{40}Ca(t,p)$-^{42}Ca(g.s.). The calculated curves are multiplied by the factor N. The data are from Ref. 24. Symbols: —, $(2p_{3/2})^2$ N=1.7; ---, $(2p_{3/2})^2$, $(2p_{1/2})^2$, $(1f_{7/2})^2$, $(1f_{5/2})^2$ N=4.0.

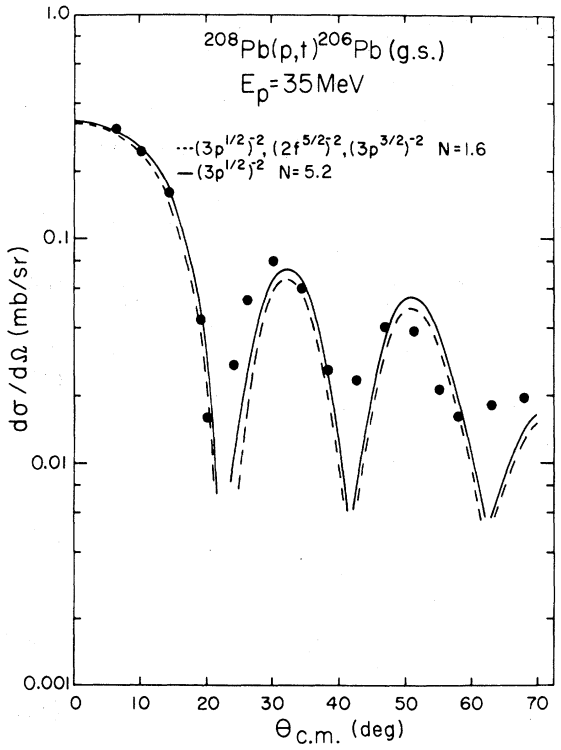

FIG. 4. Differential cross section for ^{208}Pb(p,t)-^{206}Pb(g.s.). The calculated cross sections are multiplied by the factor N. The data are from Ref. 25. Symbols: ---, $(3p_{1/2})^{-2}$, $(2f_{5/2})^{-2}$, $(3p_{3/2})^{-2}$ $N=1.6$; —, $(3p_{1/2})^{-2}$ $N=5.2$.

cesses.[14-17] However, the studies use a zero-range or no-recoil approach. In the work of this paper a formalism has been used which allows an exact evaluation of the DWBA integral and which allows explicit inclusion of multiple two-particle configurations.

It was found in Ref. 27 that using a large basis greatly increased the strength of the cross section in heavy-ion two-nucleon transfer. The size of the configuration space allowed here was restricted by considering only the major shell above (or below) the doubly closed shell nuclei involved. In the case of ^{208}Pb$(p,t)^{206}$Pb, only three of the six possible two-hole configurations were used. These three, however, give 97% of the wave function that results when the full major shell is included.[18] It would thus be strongly expected that the use of all six would have little or no effect on the calculations presented here.

It should also be pointed out that a more complete treatment of the nucleon-nucleon hard core potential in Ref. 28 found a decrease in the transition strength for (d,p) reactions. Using this more complete treatment in the work of this paper might thus reduce the size of the calculated cross sections.

With the above points in mind, it is the conclusion of this work that the theory tends to (1) predict cross sections which correctly give the forward angle shape but fall off too rapidly; and (2) tend to predict too small a strength but not by large amounts except for ^{42}Ca.

The shape of the cross section is essentially independent of the configurations used. This is seen in the results of the last section and is also seen by comparing the shapes of the form factors [$V(r_{HR})$'s of Eq. (A10)] that enter the calculations. That is, they have almost the same shape independence of the two-nucleon configuration. This is also claimed in Ref. 1. It would thus seem that the only number relevant for two-particle spectroscopy is the normalization. The independence of the shape of the cross section to the configuration space used would indicate that the too rapid falloff of the calculations would not be improved by a larger wave function. This may indicate that the shape can be improved only by including multistep processes.

The author would like to acknowledge very useful conversations with D. Robson, F. Petrovich, J. Philpott, and K. Kemper. Thanks also go to D. Robson for reading the manuscript.

APPENDIX

The expression used to numerically calculate the differential cross section is given here:

$$\frac{d\sigma_{pt}}{d\Omega}=[4(4\pi)^4]^{-1}E_p^{cm-1}E_t^{cm-1}k_tk_p^{-1}\hat{j}_p^{-2}\hat{j}_t^{-2}H(\theta), \tag{A1}$$

with

$$H(\theta)=\sum_p\sum_{\nu\geq 0}(2-\delta_{\nu 0})\left|C(T_R1T_T;N_R1N_T)\sum_{\tilde{\mathcal{L}}\,\tilde{l}}\hat{\tilde{\mathcal{L}}}^2\hat{\tilde{l}}^2\sum_{L_t}(-)^{L_t}\hat{L}_tI^{p\nu}_{L_tL_t}P^{\nu}_{L_t}(\cos\theta)\right|^2, \tag{A2}$$

$$I_{L_t}^{p\nu} = \hat{\tilde{l}}^{-1}\hat{p}^{-1} \sum_{L_p \Lambda_t \Lambda_p \bar{L}} (-)^{\Lambda_p} \hat{L}_p \hat{\bar{L}}^2 \hat{\Lambda}_t \hat{\Lambda}_p C(L_t L_p p; \nu 0 \nu) C(\Lambda_t \bar{L} L_t; 000) C(\Lambda_p \bar{L} L_p; 000) W(L_p L_t \Lambda_p \Lambda_t; p\bar{L})$$

$$\times \sum_{\lambda_1 \lambda_2} N_{\bar{L}\tilde{\mathfrak{L}}\tilde{l} L_p L_t}^{p \lambda_1 \lambda_2} \begin{pmatrix} 2 & \tilde{l} \\ 2 & \lambda_1 \end{pmatrix}^{1/2} \begin{pmatrix} 2 & \tilde{\mathfrak{L}} \\ 2 & \lambda_2 \end{pmatrix}^{1/2} \begin{Bmatrix} p & \tilde{l} & \tilde{\mathfrak{L}} \\ \Lambda_p & (\tilde{l} - \lambda_1) & \lambda_2 \\ \Lambda_t & \lambda_1 & (\tilde{\mathfrak{L}} - \lambda_2) \end{Bmatrix} C(\tilde{\mathfrak{L}} - \lambda_2 \lambda_1 \Lambda_t; 000) C(\tilde{l} - \lambda_1 \lambda_2 \Lambda_p; 000), \tag{A3}$$

$$N_{\bar{L}\tilde{\mathfrak{L}}\tilde{l} L_p L_t}^{p \lambda_1 \lambda_2} = \sum_{n_p n_t} a_{n_p L_p}^{(+)} a_{n_t L_t}^{(-)} M_{\bar{L}\tilde{\mathfrak{L}}\tilde{l}}^{p}(k_{n_p}, k_{n_t}) \left(-\frac{m_R}{m_T} k_{n_p}\right)^{\lambda_2} \left(-\frac{m_p}{m_t} k_{n_t}\right)^{\lambda_1} k_{n_p}^{(\tilde{l} - \lambda_1)} k_{n_t}^{(\tilde{\mathfrak{L}} - \lambda_2)}, \tag{A4}$$

$$M_{\bar{L}\tilde{\mathfrak{L}}\tilde{l}}^{p}(k_{n_p}, k_{n_t}) = \sum_{\tilde{n}\tilde{n}^t} K_{\tilde{n}^t \tilde{n}}^{\tilde{l}} \left[\int_{-1}^{+1} F_{\tilde{l}\tilde{n}^t}(q_1) G_{\tilde{\mathfrak{L}}\tilde{l}\tilde{n}}^{p}(q_2) P_{\bar{L}}(\mu)\, d\mu \right], \tag{A5}$$

$$\mu = \hat{\vec{k}}_{n_p} \cdot \hat{\vec{k}}_{n_t}, \tag{A6}$$

$$F_{\tilde{l}\tilde{n}^t}(q_1) = 4\pi \left[\int_0^\infty r_{pH}^2 dr_{pH}\, j_{\tilde{l}}(q_1 r_{pH}) \overline{V}_{\tilde{l}\tilde{n}^t}(r_{pH}) \right] \Big/ q_1^{\tilde{l}}, \tag{A7}$$

$$G_{\tilde{\mathfrak{L}}\tilde{l}\tilde{n}}^{p}(q_2) = 4\pi \left[\int_0^\infty r_{HR}^2 dr_{HR}\, j_{\tilde{\mathfrak{L}}}(q_2 r_{HR}) V_{\tilde{\mathfrak{L}}\tilde{l}\tilde{n}}^{p}(r_{HR}) \right] \Big/ q_2^{\tilde{\mathfrak{L}}}, \tag{A8}$$

$$\overline{V}_{\tilde{l}\tilde{n}^t}(r_{pH}) = \sum_{\tilde{n}_1^t \tilde{n}_2^t} (a_{\tilde{n}_1^t} a'_{\tilde{n}_2^t} + a'_{\tilde{n}_1^t} a_{\tilde{n}_2^t}) \langle \tilde{n}^t \tilde{l}, \tilde{N}^t \tilde{l}, 0 \mid \tilde{n}_1^t 0, \tilde{n}_2^t 0, 0 \rangle u_{\tilde{N}^t \tilde{l}}^{\text{H.O.}}(r_{pH}), \tag{A9}$$

$$V_{\tilde{\mathfrak{L}}\tilde{l}\tilde{n}}^{p}(r_{HR}) = \sum_{\tilde{n}_1 \tilde{n}_2 \tilde{N}} \sum_{n_1 l_1 j_1} \sum_{n_2 l_2 j_2} A_{n_1 n_2 l_1 l_2}^{j_1 j_2 p} \hat{j}_1 \hat{j}_2 \hat{p} \begin{Bmatrix} l_1 & \frac{1}{2} & j_1 \\ l_2 & \frac{1}{2} & j_2 \\ p & 0 & p \end{Bmatrix} a_{\tilde{n}_1} a_{\tilde{n}_2} \langle \tilde{n}\tilde{l}, \tilde{N}\tilde{\mathfrak{L}}, p \mid \tilde{n}_1 l_1, \tilde{n}_2 l_2, p \rangle [1 + (-1)^{\tilde{l}}]$$

$$\times [2(1 + \delta_{n_1 n_2} \delta_{l_1 l_2} \delta_{j_1 j_2})]^{-1/2} u_{\tilde{N}\tilde{\mathfrak{L}}}^{\text{H.O.}}(r_{HR}), \tag{A10}$$

and

$$K_{\tilde{n}^t \tilde{n}}^{\tilde{l}} = \int_0^\infty dr_{n_1 n_2} r_{n_1 n_2}^2 u_{\tilde{n}\tilde{l}}^{\text{H.O.}}(r_{n_1 n_2}) \rho(r_{n_1 n_2}) u_{\tilde{n}^t \tilde{l}}^{\text{H.O.}}(r_{n_1 n_2}). \tag{A11}$$

The $u^{\text{H.O.}}$ are harmonic oscillator radial wave functions. All other quantities not previously defined are identical to those in Ref. 10.

---

*Work supported in part by the National Science Foundation by Grants Nos. NSF-GU-2612 and NSF-GP-41834X.

[1]B. F. Bayman, Nucl. Phys. A168, 1 (1971).
[2]B. F. Bayman and D. H. Feng, Nucl. Phys. A205, 513 (1973).
[3]T. Takemasa, Nucl. Phys. A220, 31 (1974).
[4]L. A. Charlton, Nucl. Phys. A241, 144 (1975).
[5]R. Drisko and F. Rybicki, Phys. Rev. Lett. 16, 275 (1966).
[6]M. Moshinsky, Nucl. Phys. 13, 104 (1959).
[7]Y. C. Tang and R. C. Herndon, Phys. Lett. 18, 42 (1965).
[8]T. K. Lim, Nucl. Phys. A129, 259 (1969).
[9]D. Robson and R. D. Koshel, Phys. Rev. C 6, 1125 (1972).
[10]L. A. Charlton, Phys. Rev. C 8, 146 (1973).
[11]L. A. Charlton and D. Robson, Florida State University Technical Report No. 5 (unpublished).
[12]M. Pignanelli *et al.*, Phys. Rev. C 10, 445 (1974).
[13]B. F. Bayman and N. M. Hintz, Phys. Rev. 172, 113 (1968).
[14]R. J. Ascuitto and N. K. Glendenning, Nucl. Phys. A183, 60 (1972).
[15]P. D. Kunz and E. Rost, Bull. Am. Phys. Soc. 17, 902 (1972).
[16]N. B. de Takacsy, Phys. Rev. Lett. 31, 1007 (1973).
[17]V. Managoli and D. Robson, Bull. Am. Phys. Soc. 19, 453 (1974).
[18]W. W. True, Phys. Rev. 168, 1388 (1968).
[19]R. D. Becchetti and G. W. Greenlees, Phys. Rev. 182, 1190 (1969).
[20]E. R. Flynn, D. D. Armstrong, J. G. Beery, and A. G. Blair, Phys. Rev. 182, 1113 (1969).
[21]H. G. Benson and G. H. Flowers, Nucl. Phys. 126,

332 (1969).
[22]S. Kahana, Phys. Rev. C 5, 63 (1972).
[23]C. W. Ma and W. W. True, Phys. Rev. C 8, 2313 (1973).
[24]J. H. Bjerregaard *et al.*, Nucl. Phys. A103, 33 (1967).
[25]W. A. Lanford, Annual Report, Cyclotron Laboratory, Michigan State University, 1972 (unpublished); W. A. Lanford and J. B. McGrory, Phys. Lett. 45B, 238 (1973).
[26]The normalization constant N is determined by requiring $\int \theta^2 d\vec{r}_{n_1 n_2} d\vec{r}_{pH} = 1$.
[27]J. Bang *et al.*, Phys. Lett. 53B, 143 (1974).
[28]J. Dobes, Nucl. Phys. A235, 199 (1974).